Naval Research Laboratory

Washington, DC 20375-5320

NRL/MR/6840--07-9055

A Design Study of a C-Band Crestatron

DAVID K. ABE
BARUCH LEVUSH

Vacuum Electronics Branch
Electronics Science and Technology Division

DAVID P. CHERNIN

SAIC
McLean, Virginia

June 8, 2007

REPORT DOCUMENTATION PAGE

Form Approved
OMB No. 0704-0188

1. REPORT DATE *(DD-MM-YYYY)*	**2. REPORT TYPE**	**3. DATES COVERED** *(From - To)*
08-06-2007	Memorandum Report	2004 – 2007

4. TITLE AND SUBTITLE

A Design Study of a C-Band Crestatron

5a. CONTRACT NUMBER

5b. GRANT NUMBER

5c. PROGRAM ELEMENT NUMBER

6. AUTHOR(S)

David K. Abe, Baruch Levush, and David P. Chernin*

5d. PROJECT NUMBER

5e. TASK NUMBER

5f. WORK UNIT NUMBER

7. PERFORMING ORGANIZATION NAME(S) AND ADDRESS(ES)

Naval Research Laboratory
4555 Overlook Avenue, SW
Washington, DC 20375-5320

8. PERFORMING ORGANIZATION REPORT NUMBER

NRL/MR/6840--07-9055

9. SPONSORING / MONITORING AGENCY NAME(S) AND ADDRESS(ES)

10. SPONSOR / MONITOR'S ACRONYM(S)

11. SPONSOR / MONITOR'S REPORT NUMBER(S)

12. DISTRIBUTION / AVAILABILITY STATEMENT

Approved for public release; distribution is unlimited.

13. SUPPLEMENTARY NOTES

*SAIC, McLean, VA

14. ABSTRACT

This memorandum presents a design study of a high power C-band Crestatron amplifier. While conventional helix traveling-wave tubes (TWTs) are operated in an exponentially growing-wave mode, the Crestatron operates in a "beating-wave" regime where three constant-amplitude voltage waves traveling at different phase velocities along the helix beat together to produce power gain. Although inherently lower in gain than a TWT, the Crestatron can produce high power rf over a surprisingly broad frequency range with very good efficiency. In our design example, CHRISTINE 1-D large-signal simulations show that a 5850 volt, 196 mA Crestatron can produce in excess of 250 W of rf power over a frequency span of 3 to 5.5 GHz. When combined with a two-stage depressed collector, the peak efficiency of the Crestatron is ~64% compared with ~50% for a TWT of similar power over this band. The Crestatron is also a higher power density device, with an estimated 40% reduction in length and 25% reduction in mass compared to the TWT. Compact, efficient, high power, high gain transmitters can be realized by combining the Crestatron with a low-noise solid-state driver in a microwave power module (MPM) configuration. Such a system has promising applications in volume- and weight-constrained platforms such as airborne pods and unmanned vehicles.

15. SUBJECT TERMS

Crestatron, TWT, Microwave power module, Vacuum electronics
Traveling-wave tube, Beating-wave, MPM

16. SECURITY CLASSIFICATION OF:			**17. LIMITATION OF ABSTRACT**	**18. NUMBER OF PAGES**	**19a. NAME OF RESPONSIBLE PERSON**
a. REPORT	**b. ABSTRACT**	**c. THIS PAGE**			David K. Abe
Unclassified	Unclassified	Unclassified	UL	23	**19b. TELEPHONE NUMBER** *(include area code)* (202) 767-0033

Contents

List of Figures

List of Tables

1 Introduction

While conventional helix traveling-wave tubes (TWTs) are operated in an exponentially growing-wave mode, there is also a mode which operates on a beating-wave principle. In this "beat-wave" regime, three constant-amplitude waves traveling at different phase velocities along the helix beat together to produce power gain. Devices operated in this mode have been termed "Crestatrons" [1].

The Crestatron has a number of potential advantages over an exponentially growing-wave TWT of comparable power. Since it relies on a beating-wave interaction, the Crestatron circuit can be considerably shorter in length relative to a TWT circuit that uses distributed interaction to produce gain. Thus, the Crestatron is a higher power density device and may be useful in applications where volume and weight are key constraints. In general, a Crestatron will have lower gain compared with a comparable power TWT. However, low gain can be viewed as an advantage, as it reduces circuit complexity, eliminates the need for severs, and minimizes the need for high circuit attenuation to control instabilities. Using a microwave power module (MPM) approach [2], total system gains of > 30 dB can be achieved by combining the Crestatron with a high-power solid-state pre-amplifier. In this distributed gain approach, the overall system noise performance benefits from the low-noise performance of the solid-state pre-amplifier while the overall system output power performance benefits from the efficiency and high power capabilities of the vacuum electronic output stage. Overall system efficiency can be further enhanced with the introduction of a multi-stage depressed collector to recover energy from the "spent" beam electrons. Finally, the shortened length of the Crestatron circuit raises the intriguing possibility of operation without an external magnetic field, leading to further weight and volume reductions in the amplifier.

To get an understanding of the physical processes involved in Crestatron operation, we can proceed as in [1] and consider a simplified case where we neglect the effects of space charge. Then, the normalized voltage V_z/V along the rf circuit may be written in terms of the three waves as

$$\frac{V_z}{V} = e^{j(\theta/C)} \left[\frac{V_1}{V} e^{\delta_1 \theta} + \frac{V_2}{V} e^{\delta_2 \theta} + \frac{V_3}{V} e^{\delta_3 \theta} \right] \tag{1}$$

where V_i/V is the normalized voltage amplitude for each wave; $\theta = 2\pi CN$; N is the structure length in wavelengths; $C = (KI/4V)^{1/3}$ is the Pierce gain parameter [3]; K is the interaction impedance of the structure; I is the beam current; and $\delta_i = x_i + jy_i,\ i = 1, 2, 3$ are the solutions of the dispersion equation [4],

$$\delta^2(j\delta + jd - b) = 0, \tag{2}$$

In Eqn. 2, d is the Pierce loss parameter [3] and b is the normalized velocity parameter,

$$b = \frac{v_0 - v_{\rm ph}}{v_{\rm ph} C} \tag{3}$$

where v_0 is the electron velocity, $v_0 = (2eV_k/m_{\rm e})^{1/2}$; V_k is the cathode voltage; $e/m_{\rm e}$ is the electron charge-to-mass ratio; and $v_{\rm ph}$ is the circuit phase velocity.

From Eqn. 1, the device length is chosen such that the three waves add constructively at the output, resulting in an efficient, compact, relatively low-gain device (10–20 dB). We can illustrate this effect using small-signal theory and some simplifying assumptions. Following [1], we let $C \to 0$ and assume b to be sufficiently large that the propagation constants, δ_i, are purely imaginary (*i.e.*,

Manuscript approved May 9, 2007.

the case where there are no exponentially growing waves). Then,

$$\begin{aligned} \delta_1 &\simeq -j/b^{1/2}, \\ \delta_2 &\simeq -jb, \\ \delta_3 &\simeq j/b^{1/2} \end{aligned} \tag{4}$$

and the normalized voltages can be expressed as

$$\frac{V_i}{V} = \frac{\delta_i^2}{(\delta_i - \delta_{i+1})(\delta_i - \delta_{i+2})}, \quad i = 1, 2, 3. \tag{5}$$

where $\delta_{i+3} = \delta_i$. Thus, the total voltage can be expressed as a sum of these three voltages, $V_z = V_1 + V_2 + V_3$; the rf power, $P_{\rm rf}$, is proportional to $V_z V_z^*$; and the gain in dB is $10 \log |(V_z/V)^2|$. Using Eqns. 4 and 5, we can plot the three normalized voltage waves as a function of longitudinal position, z, and illustrate the rf power produced by their beating, as shown in Fig. 1.

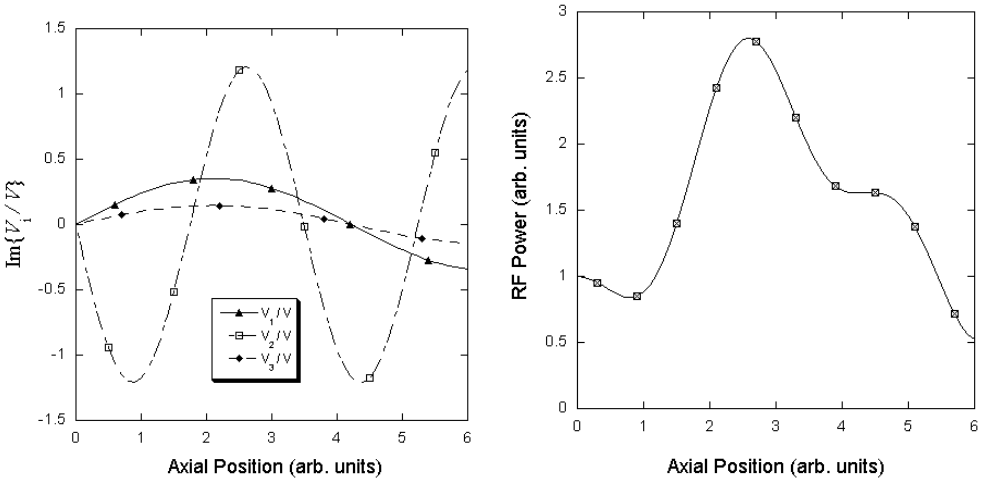

(a) (b)

Figure 1: (a) Three forward-directed voltage waves as a function of axial location as computed by Eqns. 4 and 5 for $b = 1.8$; (b) the corresponding rf power as a function of axial position.

In the following sections, we explore the potential benefits of the Crestatron by developing a conceptual amplifier design in C-band and comparing its performance with an exponentially growing-wave TWT operating at similar frequencies.

2 Design of a C-band Crestatron

To compare the performance of a Crestatron with that of a conventional, exponentially growing-wave helix TWT, we will begin the Crestatron design process using the same basic helix dimensions as described in [5], which describes a variety of growing-wave C-band helix circuit designs optimized for efficiency and linearity. The common helix parameters are summarized in Table 1.

Table 1: Common Design Parameters: Crestatron & Growing-Wave TWT

Parameter	Value
Average helix radius	0.049 in.
Helix tape width	0.014 in.
Helix tape thickness	0.006 in.
Backwall radius	0.110 in.
BeO support rod cross-section	0.02 in. $\times$ 0.061 in.

In the following sub-sections, the pitch of the Crestatron helix has been held constant and set equal to the pitch of the first stage of the growing-wave helix circuits, $\lambda_{\mathrm{h}} = 0.0395$ inches/turn.

2.1 Determination of the optimum operating voltage

To access the Crestatron regime of operation, the electron velocity must be significantly higher than the synchronous circuit phase velocity associated with the exponential-gain mode of operation. Thus, the operating voltage for beat-wave operation must be higher than that for the exponential growth mode. From [5], the nominal cathode voltage and current for the growing-wave TWT was 4800 volts and 0.146 A, respectively, with a corresponding beam perveance of 0.44×10^{-6} $\mathrm{AV}^{-3/2}$. Holding this perveance constant, the voltage and current were varied and the evolution of the rf power as a function of axial position along the helix was computed using CHRISTINE 1-D, a large-signal helix TWT code that includes beam space-charge effects [6].

The Pierce velocity parameter, b, defined in Eqn. 3 is a useful measure of the degree of asynchronism between the beam velocity and the circuit phase velocity. Values of $b > 0$ denote beam electrons streaming faster than the circuit phase velocity; this is the operating regime of interest for Crestatron mode operation.

Using the dimensions of Table 1 and a constant pitch profile of $\lambda_{\mathrm{h}} = 0.0395$ inches/turn, CHRISTINE 1-D was used to compute the small-signal rf power along the helix as a function of axial location for various beam voltages (constant perveance = 0.44 μPerv) at a drive frequency of $f = 5.25$ GHz (approximately center-band) and a drive power of $P_{\mathrm{in}} = -30$ dBm. The resulting curves are plotted in Fig. 2 (space-charge effects have been included).

As can be seen in the figure, the Crestatron regime is accessed for values of $b > 1.2$. As expected, the gain and maximum rf power is lower in the Crestatron regime than in the exponential growth regime. On the other hand, the three beating waves can reach a maximum value in a shorter distance than in the exponential growth case. The choice of operating voltage is thus a compromise between reduced circuit length and maintaining a reasonable output power and gain. From the figure, $V_k = 5.85$ kV is seen to be a promising operating voltage as it features reasonable gain, a fairly broad and flat peak, and a short interaction length (between 3 and 4 inches). The next

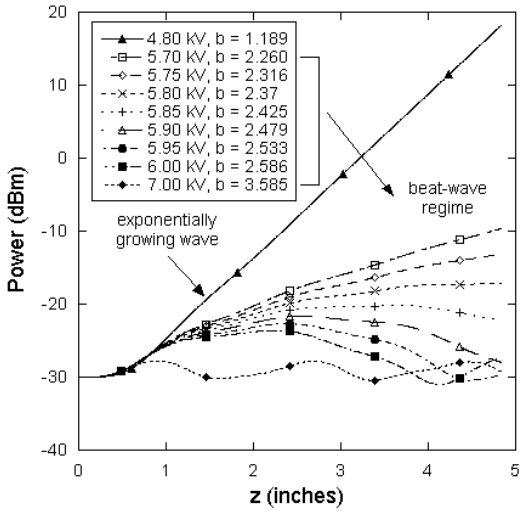

Figure 2: Small-signal rf power as a function of axial position along the helix for various beam voltages as computed by CHRISTINE 1-D. The beam perveance was held at a constant 0.44 μPerv for all cases. The basic helix parameters are as summarized in Table 1 and all plots used a constant pitch profile of $\lambda_{\mathrm{h}} = 0.0395$ inches/turn. The drive frequency was $f = 5.25$ GHz and the drive power was $P_{\mathrm{in}} = -30$ dBm.

subsection will explore the power, gain, and frequency performance of a Crestatron based on these parameters.

2.2 Choosing the Crestatron length

Based on the voltage scans of Fig. 2, a preliminary design for a Crestatron was developed; the parameters are summarized in Table 2. Note that because the Crestatron is a low-gain device, the circuit does not require a sever or high circuit attenuation for stability. These features contribute to the compact length of the device.

To determine the interaction length of the circuit, the frequency response of the circuit was simulated with CHRISTINE 1-D for an input power of -30 dBm. Figure 2.2 is a plot of the rf power as a function of axial location along the helix for a constant drive power of -30 dBm and frequencies ranging from 5 to 5.35 GHz. From the figure, a promising circuit length is $L = 3$ inches, where a compromise is struck between compact length and a peak in the output power over a reasonably broad bandwidth. The circuit performance over a variety of input powers and frequencies is evaluated with CHRISTINE 1-D in the following sub-section.

Table 2: C-band Crestatron parameters

Parameter	Value
Cathode voltage	5850 volts
Beam current	0.1964 A
Perveance	0.44×10^{-6}
Beam fill factor ($r_\mathrm{b}/r_\mathrm{h}$)	0.60
Average helix radius	0.049 in.
Helix pitch, λ_h	0.0395 in./turn
Helix tape width	0.014 in.
Helix tape thickness	0.006 in.
Backwall radius	0.110 in.
BeO support rod cross-section	0.02 in. $\times$ 0.061 in.

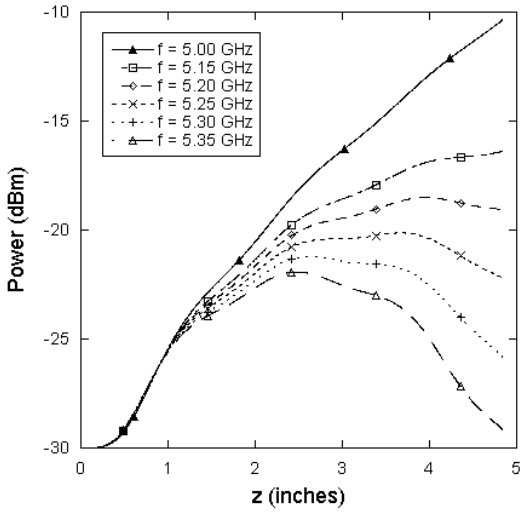

Figure 3: CHRISTINE 1-D simulations of the Crestatron small-signal rf power as a function of axial position along the helix for various frequencies (where $P_\mathrm{in} = -30$ dBm and the basic circuit parameters are summarized in Table 2).

2.3 Predicted performance of the C-band Crestatron

Using a circuit length of $L = 3$ inches and the parameters of Table 2, CHRISTINE 1-D was used to simulate the input-output response of the TWT to single-tone excitation. The resulting simulated drive and gain curves for frequencies ranging from 3 to 6 GHz are shown in Figs. 4(a) and 4(b), respectively.

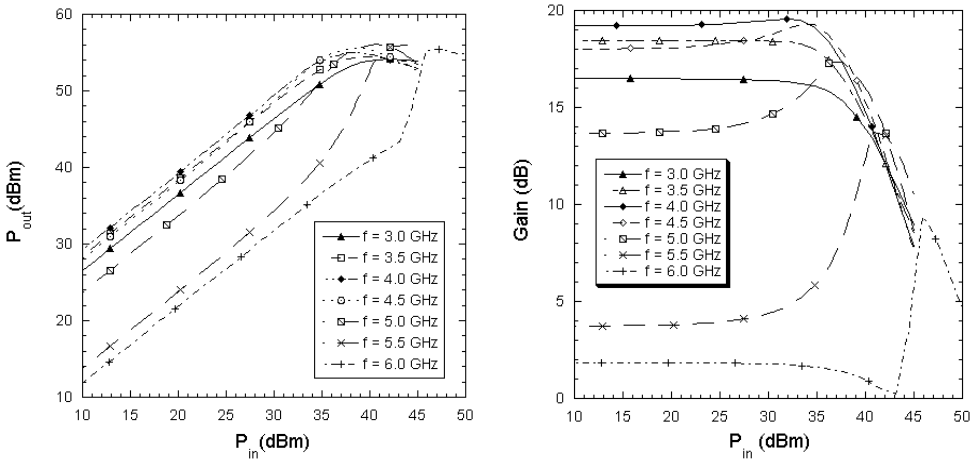

(a) (b)

Figure 4: CHRISTINE 1-D Crestatron simulations for a design using the parameters of Table 2 and a total circuit length of 3 inches. (a) Output power versus input power and (b) gain versus input power for a range frequencies.

As the frequency is increased, the small-signal gain of the Crestatron is seen to drop and gain expansion near saturation becomes increasingly pronounced. To understand these effects, we can examine at the Crestatron performance in greater detail at the two extremes of the frequency range. Figures 5(a) and 5(b) plot the beam energy as a function of axial position for a range of rf drive powers at drive frequencies of 3 and 6 GHz, respectively. From these plots, using the beam energy at the end of the circuit, we can compute the "local" value of the Pierce velocity parameter, b, from Eqn. 3 and the definition of the Pierce gain parameter, $C^3 = KI/4V$ (these values are readily obtained from the CHRISTINE 1-D simulations).

At $f = 3$ GHz, Fig. 5(a) shows that the circuit extracts energy from the beam over a wide range of drive powers and the beam velocity remains close to the synchronous condition. For this case, as seen in Fig. 6(a), b ranges from -0.2 to 1.1, and the Crestatron exhibits relatively high gain. At $f = 6$ GHz, however, Fig. 5(b) indicates that the beam-wave interaction is weak at low drive levels and the beam velocity remains high and out of synchronism with the phase velocity of the circuit wave. Here, the amplifier is operating strongly in the Crestatron regime, with $b \sim 3$, and has correspondingly low gain, as seen in Fig. 6(b). At higher drive levels – above 44 dBm – the interaction efficiency improves and the beam velocity drops closer to synchronism with the circuit wave with a corresponding increase in output power and an expansion in gain.

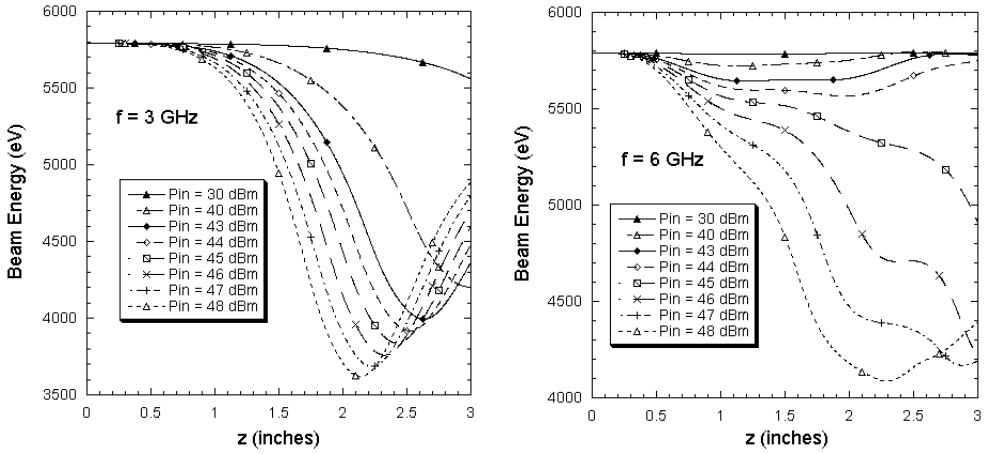

(a) (b)

Figure 5: Simulations of the $L = 3$ inch Crestatron beam energy as a function of axial position, z, for various rf input powers at (a) $f = 3$ GHz and (b) $f = 6$ GHz.

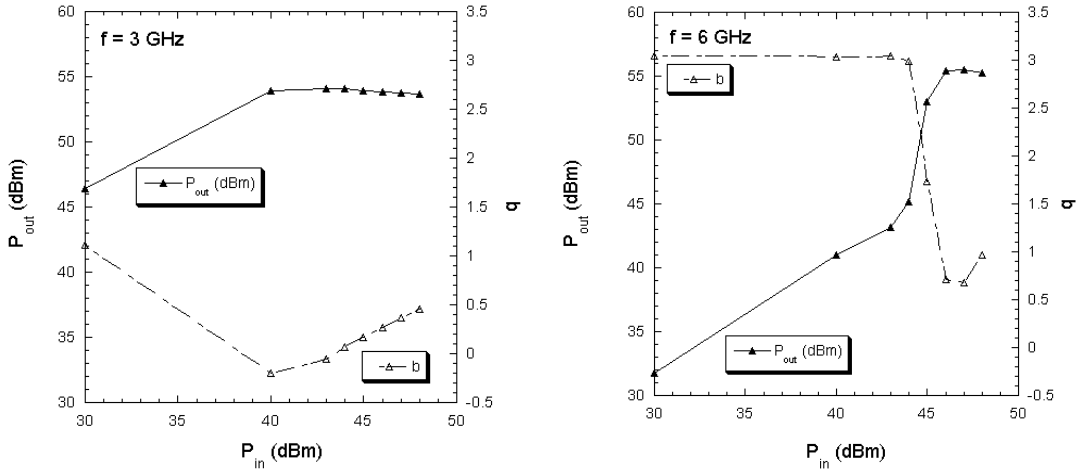

(a) (b)

Figure 6: Simulations of the $L = 3$ inch Crestatron output power and Pierce velocity parameter, b, as a function of input power for (a) $f = 3$ GHz and (b) $f = 6$ GHz.

Thus, over a wide range of frequencies and depending on the rf input drive level, the $L = 3$ inch long circuit can operate in quasi-synchronous ($-1 \leq b \leq 1$) and non-synchronous ($b > 1$) modes. This flexibility accounts for the surprisingly broad frequency response of the device at saturation. Figures 7(a) and 7(b) plot the computed rf output power and gain at saturation as a function of frequency. The simulations predict that the circuit will produce > 54 dBm (> 251 W) of output power with corresponding gains in excess of 12 dB over a 2.5 GHz frequency range. The corresponding peak electronic efficiency at saturation is good, ranging from $22 - 36\%$ over the 2.5 GHz range as seen in Fig. 7(b).

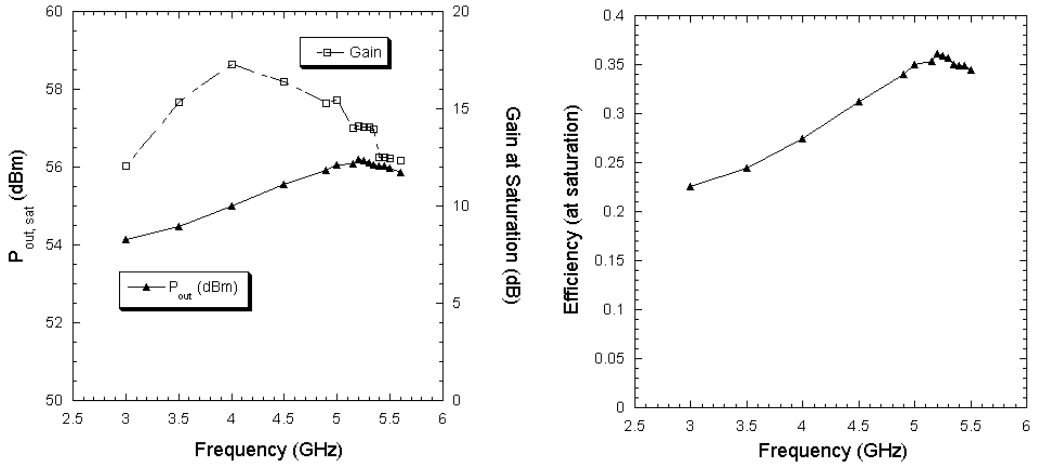

(a) (b)

Figure 7: (a) C-band Crestatron predicted output power and gain at saturation as a function of frequency; and (b) the corresponding electronic efficiency ($P_{\rm out}/V_{\rm k}I$) at saturation as a function of frequency.

3 Comparison of C-band Crestatron Performance with Exponentially Growing-Wave TWTs

3.1 Constant pitch TWT with a 3 inch long circuit length

In Sect. 2.2, the optimum Crestatron length was found to be 3 inches. As a point of comparison, we compare the performance of a constant pitch helix TWT of comparable length. The TWT parameters are summarized in Table 3.

Table 3: Exponentially growing-wave TWT parameters

Parameter	Value
Cathode voltage	4800 volts
Beam current	0.146 A
Perveance	0.44×10^{-6}
Beam fill factor ($r_\mathrm{b}/r_\mathrm{h}$)	0.50
Average helix radius	0.049 in.
Helix pitch, λ_h	0.0394 in./turn
Helix tape width	0.014 in.
Helix tape thickness	0.006 in.
Backwall radius	0.110 in.
BeO support rod cross-section	0.02 in. $\times$ 0.061 in.

Figure 8 compares the predicted performance of the Crestatron described in Table 2 with that of the constant pitch helix TWT. As seen in the figure, the Crestatron produces approximately twice the output power over an octave frequency range – as noted previously, a surprisingly wide range for a device that works on the principle of beating voltage waves. The electronic efficiency of the Crestatron is also superior to that of the TWT, with a maximum value of 36% compared to 29% for the TWT (both devices using grounded collectors). However, the Crestatron is a relatively low gain device, as seen in Fig. 8(c) which plots the saturated gain as a function of frequency for both devices. In this example, the Crestatron has a maximum gain of ~ 17 dB compared with ~ 21 dB for the TWT.

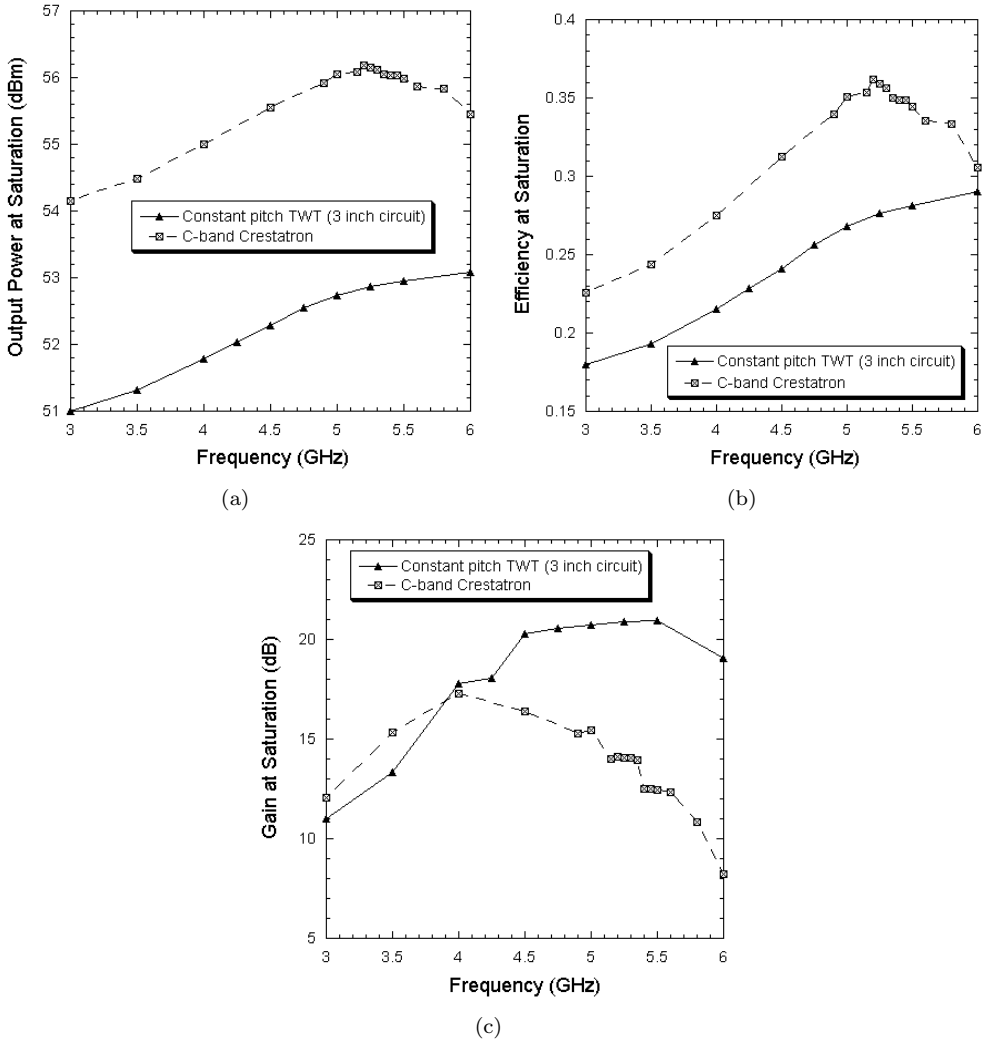

Figure 8: A comparison of the predicted performance of a constant pitch helix TWT with a circuit length of 3 inches (Table 2) and a Crestatron of comparable length (Table 3). (a) Output power at saturation as a function of frequency; (b) electronic efficiency at saturation as a function of frequency; (c) saturated gain as a function of frequency.

3.2 Comparison with a complex-gain optimized TWT

It is of greater interest, however, to compare the performance of the Crestatron with that of a conventionally-designed TWT. Such a TWT is described in [5] in sufficient detail to enable a design comparison. In particular, we compare the performance of the C-band Crestatron with that of the TWT optimized using the complex-gain goal function described in Eqns. (2) and (3) of [5]. Both the Crestatron and the TWT share common design parameters, including the same electron gun (where the beam perveance has been kept constant), helix dimensions, and vacuum envelope radius. Of course, the helix pitch and circuit length are different in the two devices. The TWT circuit consists of two helix stages separated by a sever; the second stage is velocity tapered, as shown in Fig. 9. The total length of the helix is 4.78 inches; other pertinent parameters are as shown in Table 3. The principle differences between the TWT and Crestatron designs are summarized in Table 4.

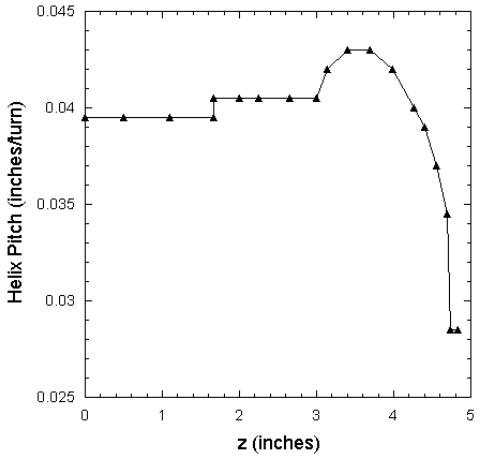

Figure 9: Helix pitch versus axial position for the complex-gain optimized TWT described in [5].

Table 4: Crestatron and TWT design differences

Parameter	Crestatron	TWT
Cathode voltage	5850 volts	4800 volts
Beam current	0.1964 A	0.146 A
Circuit length	3 inches	4.78 inches
No. of stages	1 (constant pitch)	2 (velocity-tapered)
Sever	No	Yes

Figure 10 compares the saturated output power, gain, and efficiency of the C-band Crestatron and the complex-gain optimized TWT. Over the 3 to 5.5 GHz frequency range, the Crestatron can be seen to outperform the TWT in output power production, producing rf power in the range of $54 \leq P_{\rm out} \leq 56.2$ dBm ($251 \leq P_{\rm out} \leq 417$ W), compared with a maximum of 53 dBm (300 W). The Crestatron is also more efficient, with a maximum electronic efficiency of 36% compared with 28% for the TWT; the Crestatron also does better job of maintaining a high efficiency over the band. As expected, the TWT gain is significantly higher than the gain of the Crestatron, however the latter device has less gain variation with frequency.

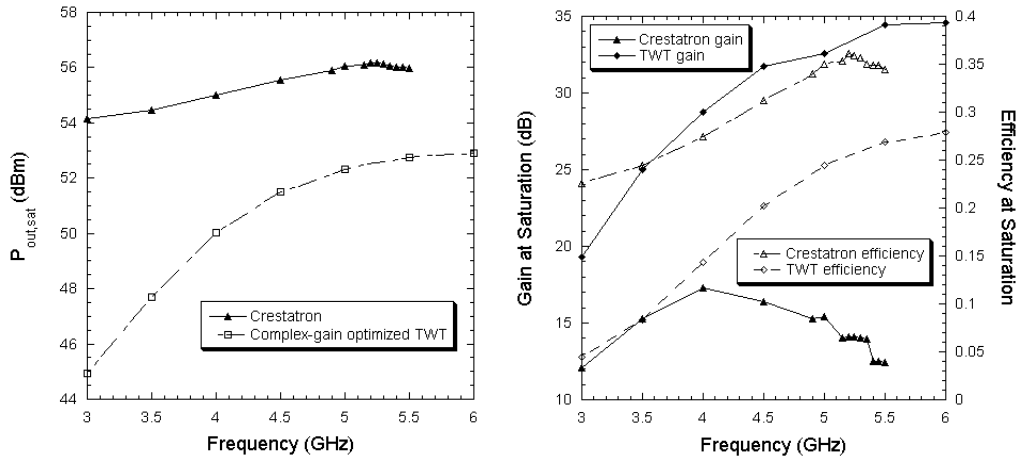

(a) (b)

Figure 10: A comparison of the predicted performance of the C-band Crestatron with the complex-gain optimized TWT of [5]. (a) Output power at saturation as a function of frequency; (b) gain and electronic efficiency at saturation as a function of frequency.

Figures 11 and 12 compare the linearity of the Crestatron with the complex-gain optimized TWT. Figure 11(a) plots the predicted output power of the two devices at the 1-dB gain compression (expansion) point as a function of frequency; note that the Crestatron produces higher output power at the 1-dB point in the frequency range of 3 to ~ 4.6 GHz. Figure 11(b) plots the frequency dependence of the predicted amplitude modulation to phase modulation (AM-PM) response of the two devices at the point of 6-dB output power backoff (OBO). As can be seen in the figure, the Crestatron exhibits a poorer AM-PM response compared with the TWT, particularly at the upper band-edge. However, the Crestatron also produces significantly higher output power at 6-dB OBO; if the Crestatron operating point was further reduced to match the output power of the TWT, the AM-PM response would improve.

Figure 11 examines linearity issues in the Crestatron and the TWT in response to single-tone input. To study the amplifier responses to multi-tone inputs, we used the multiple frequency capability of CHRISTINE 1-D to compute the third- and fifth-order carrier-to-intermodulation products (C3IM and C5IM, respectively) in response to two-tone, equal amplitude inputs at the relatively wide frequency separation of 50 MHz (drive frequencies of $f_1 = 5.0$ GHz and $f_2 = 5.05$ GHz). The CIM results are plotted in Fig. 12 as a function of rf output power.

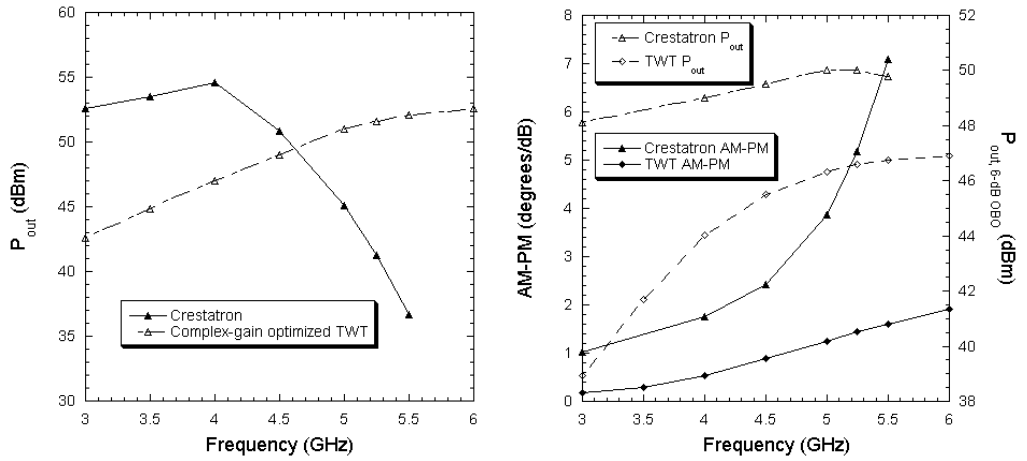

(a) (b)

Figure 11: A comparison of the linearity of the C-band Crestatron and complex-gain optimized TWT: (a) output power at the 1-dB gain compression/expansion point as a function of frequency; (b) gain and electronic efficiency at satmuration as a function of frequency.

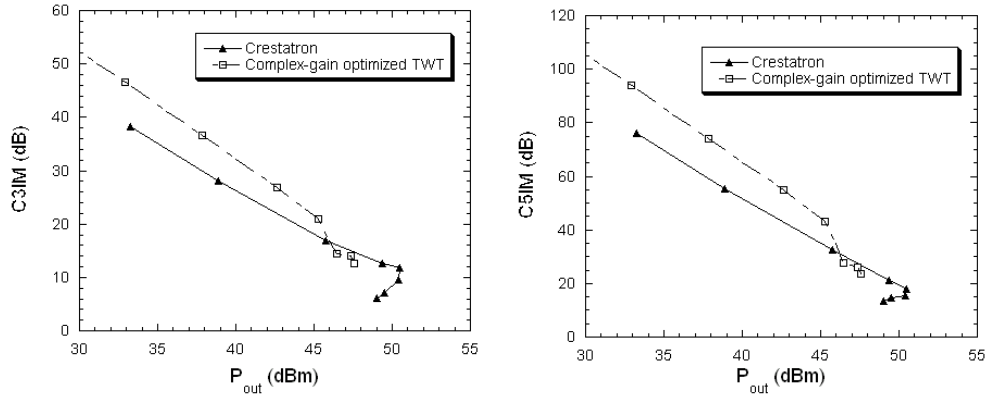

(a) (b)

Figure 12: A comparison of the response of the C-band Crestatron and complex-gain optimized TWT to a two-tone input ($f_1 = 5.0$ GHz, $f_2 = 5.05$ GHz; each frequency driven with equal power: (a) C3IM versus output power; (b) C5IM versus output power.

As seen in Figs. 12(a) and 12(b), for output powers less than 46-dBm, the C3IM and C5IM characteristics of the TWT is better than that of the Crestatron. For example, if an application required a C3IM performance of 20-dB, the output power of the Crestatron would have to be reduced by -1.7 dB compared with the TWT. On the other hand, the Crestatron can produce significantly higher output power – a maximum of about 50.5-dBm with a corresponding C3IM of about 11.7-dB.

It should be noted that this design exercise is primarily focused on optimizing Crestatron parameters to increase efficiency and power density rather than linearity. A full linearization study is beyond the scope of this report.

4 Crestatron Performance with Multi-Stage Depressed Collectors

An advantage of vacuum electronic devices in general is the possibility to increase overall efficiency through the recovery of some of the energy in the "spent" beam, *i.e.* the residual energy in the beam after the rf energy has been extracted in the output circuit. This energy recovery can be accomplished using a depressed collector, where the voltage of one or more electrodes in the collector are reduced (depressed) below the body potential of the collector (usually held at ground for safety reasons).

Figure 13 is a plot of the collector current as a function of the voltage bias on the collector for the Crestatron design of Sect. 2.2 under saturated rf drive conditions $P_{\rm in,sat} = 42$ dBm at $f = 5.25$ GHz.

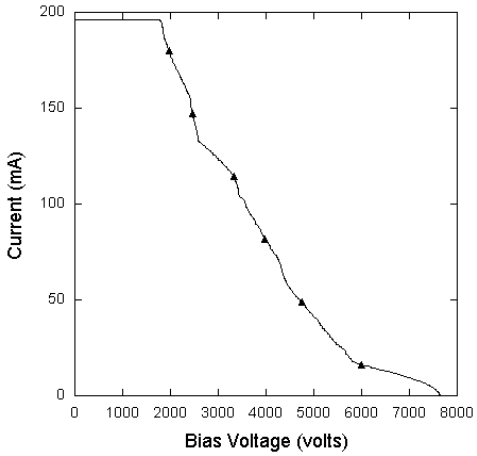

Figure 13: Collector current versus collector bias voltage for the Crestatron design of Sect. 2.2 ($P_{\rm in,sat} = 42$ dBm, $f = 5.25$ GHz).

To demonstrate the benefits of collector depression, we computed the total efficiency for the Crestatron as a function of a single-stage depressed collector bias voltage at a drive frequency of $f = 5.25$ GHz using CHRISTINE 1-D. The results are summarized in Fig. 14(a). With a grounded collector, the maximum efficiency is $\sim 35\%$; a properly biased single-stage depressed collector can increase the maximum efficiency to $> 50\%$. Using the optimization features in CHRISTINE 1-D, the optimum collector bias voltage was found to be -2944 volts with a corresponding total efficiency of $\sim 51\%$ as seen in Fig. 14(b).

Table 5: Optimized 2-stage collector voltages: Crestatron and TWT

	Crestatron	TWT
Stage #1 bias	-1777 volts	-2200 volts
Stage #2 bias	-4029 volts	-3000 volts

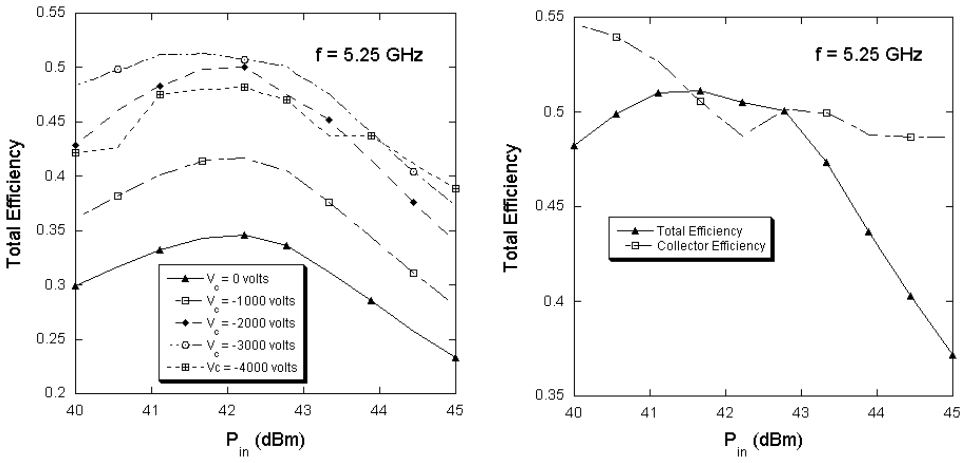

(a) (b)

Figure 14: Total Crestatron efficiency using a single-stage depressed collector at a drive frequency of $f = 5.25$ GHz. (a) Total efficiency versus $P_{\rm in}$ for various voltage biases; (b) total efficiency and collector efficiency versus $P_{\rm in}$ for the optimal collector bias, $V_{\rm c} = -2944$ volts.

The addition of a second depressed collector stage can further increase the total efficiency of the amplifier. Table 5 compares the optimized collector stage voltages for the Crestatron and exponentially growing-wave TWT. The peak total efficiencies of the two amplifiers are plotted as a function of frequency in Fig. 15. As seen in the figure, the two-stage depressed collector enables the Crestatron to achieve a peak efficiency of $\sim 64\%$ compared with 50% for the TWT.

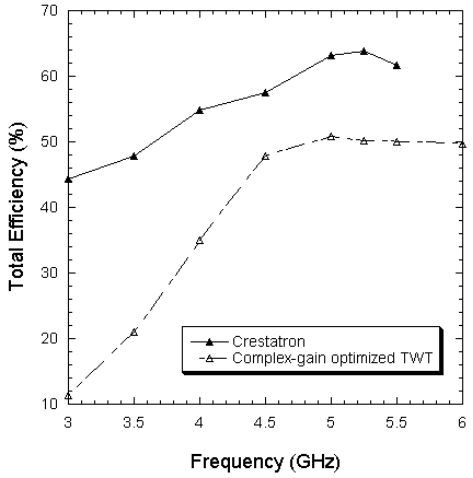

Figure 15: CHRISTINE 1-D predicted total efficiencies for the C-band Crestatron and complex-gain optimized TWT with optimized two-stage depressed collectors (collector biases are summarized in Table 5).

5 Magnetic Circuit Mass Reduction

Previous sections have discussed the significant reduction in circuit length that is possible with the beating-wave Crestatron circuit compared to the exponentially growing-wave helix TWT circuit. In our C-band examples, we found an almost 40% reduction in length for the Crestatron over the complex-gain optimized TWT (3 inches and 4.78 inches, respectively, as summarized in Table 4). We will use these two examples to further illustrate mass and volume savings using the Crestatron circuit.

The magnetic circuit required to guide the electron beam through the helix circuit is one of the largest contributors to the overall weight of the amplifier. The complex-gain optimized TWT of [5] uses a periodic permanent magnet (PPM) focused stack. The stack consists of 40 ring magnets separated by thin iron pole-pieces. The rare-earth permanent magnet material is samarium cobalt with a mass density of ~ 8.5 g/cm^3; the individual permanent magnet rings have an outer diameter of 0.55 inches (1.4 cm), inner diameter of 0.16 inches (0.4 cm), and a width of 0.1 inches (0.25 cm). The iron pole-pieces have a similar outer and inner diameter and a width of 0.04 inches (~ 0.1 cm). Thus, the total weight of the magnet system for the TWT is approximately 111 g. In contrast, assuming the same magnet dimensions for the Crestatron circuit, the magnet system mass is about 83 g, or about 75% of the mass of the TWT system. Keeping these same dimensions, the volume of the circuits scale linearly with the circuit length: about 4.35 cm^3 and 6.93 cm^3 for the Crestatron and complex-gain optimized TWT circuits, respectively. These parameters are summarized in Table 6 below.

Table 6: Mass and volume comparison: Crestatron vs. TWT

	Crestatron	TWT
Circuit length	7.62 cm	12.14 cm
Magnet system mass	83 g	111 g
Circuit volume	4.35 cm^3	6.93 cm^3

As a final comment, we note that the short length of the Crestatron circuit raises the possibility of device designs that require minimal or no magnetic focusing at all. As mentioned in [1], such devices would require an electron gun design that focuses a convergent beam at the center of the circuit. Such a beam would have a diverging radius as it propagated through the structure, expanding under its own space-charge forces. The beam dynamics would be further complicated by beam bunching induced by the rf drive.

6 Summary

The operation of a linear beam amplifier helical circuit in the beating-wave ("Crestatron") mode can lead to a significant reduction in the length, mass, and volume of the device compared with an exponentially growing-wave TWT circuit of comparable power. Although inherently lower in gain than a TWT, the Crestatron can produce high power rf over a surprisingly broad frequency range with very good efficiency. For example, CHRISTINE 1-D large-signal simulations of a C-band Crestatron indicate that a 5850 volt, 196 mA device can produce in excess of 250 W (> 54 dBm) over a frequency span of 3 to 5.5 GHz. When combined with a two-stage depressed collector, the peak efficiency of the Crestatron is $\sim 64\%$ compared with $\sim 50\%$ for a TWT of similar power over this band. The Crestatron is also a higher power density device, with an estimated 40% reduction in length and 25% reduction in mass compared to the TWT. Compact, efficient, high power, high gain transmitters can be realized by combining the Crestatron with a low-noise solid-state driver in a microwave power module (MPM) configuration. Such a system has promising applications in volume- and weight-constrained platforms such as airborne pods and unmanned vehicles.

References

[1] J. E. Rowe, "Theory of the Crestatron: A forward-wave amplifier," *Proc. IRE*, vol. 47, pp. 536–545, April 1959.

[2] C. R. Smith, C. M. Armstrong, and J. Duthie, "The Microwave Power Module: A versatile RF building block for high-power transmitters," *Proc. IEEE*, vol. 87, no. 5, pp. 717–737, May 1999.

[3] J. .R. Pierce, *Traveling-Wave Tubes*, Princeton, NJ: D. Van Nostrand Company, Inc., 1950.

[4] B. N. Basu, *Electromagnetic Theory and Applications in Beam-Wave Electronics*, Singapore: World Scientific, 1996.

[5] D. K. Abe, B. Levush, T. M. Antonsen, Jr., D. R. Whaley, and B. G. Danly, "Design of a linear C-band helix TWT for digital communications experiments using the CHRISTINE suite of large-signal codes," *IEEE Trans. Plasma Sci.*, vol. 30, no. 3, pp. 1053–1062, June 2002.

[6] T. M. Antonsen, Jr. and B. Levush, "CHRISTINE: A multi-frequency parametric simulation code for traveling-wave tube amplifiers," NRL Tech. Rep. No. 97-9845, 1997.